Maximum Likelihood Estimators in Magnetic Resonance Imaging

M. Dylan Tisdall[1], M. Stella Atkins[1], and R.A. Lockhart[2]

[1] School of Computing Science, Simon Fraser University, Burnaby BC V5A 1S6
[2] Department of Statistics & Actuarial Science, Simon Fraser University, Burnaby BC V5A 1S6

Abstract. Images of the MRI signal intensity are normally constructed by taking the magnitude of the complex-valued data. This results in a biased estimate of the true signal intensity. We consider this as a problem of parameter estimation with a nuisance parameter. Using several standard techniques for this type of problem, we derive a variety of estimators for the MRI signal, some previously published and some novel. Using Monte Carlo experiments we compare the estimators we derive with others previously published. Our results suggest that one of the novel estimators we derive may strike a desirable trade-off between bias and mean squared error.

1 Introduction

Greyscale MR images are normally produced by taking the pixel-wise magnitude of a complex-valued image with zero-mean complex additive white noise. The magnitude operation performed on this data produces an image with a Rician noise distribution [1,2]. This distribution has a spatially varying bias that is inversely related to signal strength, and thus reduces image contrast. In order to reduce the bias of this signal estimate, a variety of approaches have been presented in the literature. The first major group assumes pixels are independent, and attempts to construct a less-biased estimator for the signal value using only information recorded at a single location[1,3,4,5,6,7,8]. The second group assumes that pixels are related either in signal or phase values and uses inference between neighbouring pixels in order to estimate pixel values [9,10,11,12,13,14,15,16].

In this work, we will focus on the first group. In particular, we are interested in how the notion of a nuisance parameter can be used to construct a variety of different estimators from the established model of the MRI data. As we will see, in the majority of MR imaging situations, only one of the two parameters is of interest. The choice of how these parameters' effects are separated is fundamental in determining what sort of estimator will be produced. However, despite the rich statistical literature on estimation with nuisance parameters, the notion does not seem common in the literature on MRI signal magnitude estimation [17,18,19,20]. In this work, we will attempt to employ some of the variety of techniques available for maximum likelihood estimation with a nuisance parameter.

N. Karssemeijer and B. Lelieveldt (Eds.): IPMI 2007, LNCS 4584, pp. 434–445, 2007.

In doing so, we will derive some estimators that are previously published as well as new estimators.

To begin, in section 2 we introduce the model we will use for the MRI data. In section 3 we proceed to derive a variety of estimators using the maximum likelihood framework. In section 4 we describe some other estimators for this problem that have been presented in the MRI literature but do no arise from the maximum likelihood estimator. Finally, in section 5 we compare all of the estimators. Since closed form expressions for the bias and mean squared error (MSE) are not available for all of the estimators we derive, our comparison is based on Monte Carlo experiments using clinically realistic parameters.

2 MRI Data

For many clinically useful pulse sequences, the recorded MRI data f can be well described at each pixel as a complex-valued signal with magnitude s and phase ϕ, summed with two independent noises q_r and q_i which are both drawn from the zero-mean normal distribution $\mathcal{N}(0, \sigma)$ with σ fixed for all pixels. The two noises are aligned in the complex plane such that q_r is noise in the real direction and q_i is noise in the imaginary direction. Thus, for a given pixel we have [3]

$$f = s\exp(\mathrm{i}\phi) + q_r + \mathrm{i}q_i\,. \tag{1}$$

Since we are assuming that each pixel is independent and that the values of s and ϕ and unrelated between pixels, we can model each pixel independently with $f = a + \mathrm{i}b$ and the multinormal distribution

$$p(a, b; s, \phi, \sigma) = \frac{1}{2\pi\sigma^2}\exp\left(-\frac{(a - s\cos(\phi))^2 + (b - s\sin(\phi))^2}{2\sigma^2}\right). \tag{2}$$

Converting this to polar coordinates $f = r\exp(\mathrm{i}\theta)$, where we will find most of our work more natural, we get

$$p(r, \theta; s, \phi, \sigma) = \frac{r}{2\pi\sigma^2}\exp\left(-\frac{s^2 + r^2 - 2sr\cos(\theta - \phi)}{2\sigma^2}\right). \tag{3}$$

Since multiple excitations are often used in order to repeat measurements, we will use a_i and b_i to represent the measurements from the i^{th} excitation and $\boldsymbol{a}$ and $\boldsymbol{b}$ to represent the vectors of real and imaginary measurements at a given location. Similarly, we will use r_i and θ_i for the i^{th} excitation and $\boldsymbol{r}$ and $\boldsymbol{\theta}$ to represent the vectors of polar measurements. Finally, we will simplify notation in some places by using $A = \sum_{i=1}^{n} a_i$ and $B = \sum_{i=1}^{n} b_i$.

In the majority of clinical imaging cases, we desire to display a greyscale image where the intensities represent the value of s. This leaves ϕ, a nuisance parameter required to complete the model but not of interest in producing our images. We will be given n replicated samples from each pixel and asked to produce an estimate of s from these values.

Note that for the purposes of this paper, we will assume that σ is known. In practice σ will usually be estimated either from a region of air where it is known that $s = 0$ or from the aggregate of image pixels. In the latter case, we take advantage of the fact that, for the pulse sequences we will consider, σ is the same for all pixels in the image and so it is relatively easy to estimate given more than one replication at each pixel.

3 Maximum Likelihood Estimators with Nuisance Parameters

If we desire to estimate $s\cos\phi$ and/or $s\sin\phi$, then the MLE is a good approach. To find this estimate given the likelihood function $L(s, \phi; \boldsymbol{a}, \boldsymbol{b})$, we set the score function with respect to each parameter equal to zero, substitute in the measured values of $\boldsymbol{a}$ and $\boldsymbol{b}$, and then solve the system

$$\frac{\partial}{\partial(s\cos\phi)} \log L(s, \phi; \boldsymbol{a}, \boldsymbol{b}) = 0 \tag{4}$$

$$\frac{\partial}{\partial(s\sin\phi)} \log L(s, \phi; \boldsymbol{a}, \boldsymbol{b}) = 0\,. \tag{5}$$

This produces an unbiased estimate of $(s\cos\phi, s\sin\phi)$. However, unbiasedness does not apply when we attempt to estimate s alone. Due to the nonlinear change of parameters between $(s\cos\phi, s\sin\phi)$ and (s, ϕ), there is not one estimator of s that can be easily justified theoretically. In this section we will consider several different approaches to estimating s without ϕ. Some of the estimators derived are previously published, while some are new to the MRI literature.

3.1 Maximum Likelihood Estimate

Let $(\hat{s}_{\mathrm{ML}}, \hat{\phi}_{\mathrm{ML}})$ be the MLE of (s, ϕ) computed by solving

$$\frac{\partial}{\partial s} \log L(s, \phi; \boldsymbol{r}, \boldsymbol{\theta}) = 0 \tag{6}$$

$$\frac{\partial}{\partial \phi} \log L(s, \phi; \boldsymbol{r}, \boldsymbol{\theta}) = 0\,. \tag{7}$$

If we take $\hat{s}_{\mathrm{ML}}$ as our estimate of s alone, this is also called the maximum likelihood estimate. This is the same as substituting $\hat{\phi}_{\mathrm{ML}}$ into the score function for s, and then solving the equation

$$\frac{\mathrm{d}}{\mathrm{d}s} \log L(s; \hat{\phi}_{\mathrm{ML}}, \boldsymbol{r}, \boldsymbol{\theta}) = 0\,. \tag{8}$$

Noting that $\hat{s}_{\mathrm{ML}}$ is just the magnitude image computed at each pixel from the average of the excitations, one should not be surprised to find this estimator is

biased since it has a Rician distribution as discussed in section 1. The bias and MSE of this estimator are

$$E[\hat{s}_{\mathrm{ML}} - s] = \frac{\sqrt{2\pi}\sigma}{2\sqrt{n}} {}_1\mathrm{F}_1\left(-\frac{1}{2}; 1; -\frac{ns^2}{2\sigma^2}\right) - s \tag{9}$$

$$E[(\hat{s}_{\mathrm{ML}} - s)^2] = 2(s^2 + \sigma^2/n) - \frac{s\sqrt{2\pi}\sigma}{\sqrt{n}} {}_1\mathrm{F}_1\left(-\frac{1}{2}; 1; -\frac{ns^2}{2\sigma^2}\right), \tag{10}$$

with ${}_1\mathrm{F}_1$ being the confluent hypergeometric function. Despite the non-zero bias, this is the most prevalent form of MR signal estimate, being commonly known as the 'magnitude image' in MRI.

For this problem, we also find that the maximum profile likelihood estimate is the same as the maximum likelihood estimate [18]. The profile likelihood for s is defined as

$$L_p(s; \boldsymbol{r}, \boldsymbol{\theta}) = \max_{\phi} L(s, \phi; \boldsymbol{r}, \boldsymbol{\theta}) \tag{11}$$

We find that $\hat{s}_{\mathrm{ML}} = \max_s L_p(s; \boldsymbol{r}, \boldsymbol{\theta})$ by noting the maximum value of $L(s, \phi; \boldsymbol{r}, \boldsymbol{\theta})$ with s fixed is independent of the choice of s. Thus, for the problem of estimating the MRI signal, the $\hat{s}_{\mathrm{ML}}$ can be thought of as either the maximum likelihood estimate or the maximum profile likelihood estimate.

3.2 Maximum Marginal Likelihood Estimate

We note that equation (3) can be marginalized with respect to θ to produce

$$\begin{aligned} p(r; s, \phi) &= \int_{-\pi}^{\pi} p(r, \theta; s, \phi, \sigma)\, \mathrm{d}\theta \\ &= \frac{r}{2\pi\sigma^2} \exp\left(-\frac{s^2 + r^2}{2\sigma^2}\right) \int_{-\pi}^{\pi} \exp\left(\frac{sr\cos(\theta - \phi)}{\sigma^2}\right) \mathrm{d}\theta\,. \end{aligned} \tag{12}$$

Using the identity $\int_{-\pi}^{\pi} \exp(z\cos(\theta))\, \mathrm{d}\phi = \frac{1}{2\pi} \mathrm{I}_0(z)$, where $\mathrm{I}_0(z)$ is the zeroth-order modified Bessel function, we can rewrite this as

$$p(r; s, \phi) = \frac{r}{\sigma^2} \exp\left(-\frac{s^2 + r^2}{2\sigma^2}\right) \mathrm{I}_0\left(\frac{sr}{\sigma^2}\right). \tag{13}$$

We can see that by performing this marginalization we have removed the dependence on ϕ since it does not appear anywhere on the right side of the equation. Thus, if we measure only the magnitude and not the phase (or simply ignore the measured phase) then ϕ has no effect on our magnitude measurement. We can use this probability to produce a marginal likelihood function, which can then be maximized to produce an estimate of s [18].

This procedure is exactly the one employed by Sijbers *et al.*, although in this previous work the justification for discarding the phase was the assumption that bias correction was being performed given only a magnitude image [6]. Regardless

of how we justify the marginalization, given that we have n independent measurements of this value, we can follow a similar derivation and write

$$\begin{aligned} p(\boldsymbol{r}; s) &= \prod_{i=1}^{n} p(r_i; s) \\ &= \prod_{i=1}^{n} \frac{r_i}{\sigma^2} \exp\left(-\frac{s^2 + r_i^2}{2\sigma^2}\right) \mathrm{I}_0\left(\frac{s r_i}{\sigma^2}\right) . \end{aligned} \tag{14}$$

From this we can find

$$\frac{\mathrm{d}}{\mathrm{d}s} \log L(s; \boldsymbol{r}) = \frac{1}{\sigma^2} \left(\sum_{i=1}^{m} r_i \frac{\mathrm{I}_1\left(\frac{s r_i}{\sigma^2}\right)}{\mathrm{I}_0\left(\frac{s r_i}{\sigma^2}\right)} - ns \right) . \tag{15}$$

Setting this equal to zero produces an equation whose solutions have been studied previously using catastrophe theory [6]. The basic result of this previous work is that the maximum marginal likelihood estimate of s is 0 when $\sum_{i=1}^{n} r_i^2 \leq 2n\sigma^2$. Otherwise, there is one positive maximum which can be found numerically.

3.3 Maximum Integrated Likelihood Estimate

A very similar result to the above is produced if, instead of marginalizing out $\boldsymbol{\theta}$, we choose a uniform distribution on the range $(-\pi, \pi]$ as a prior for ϕ. The choice of a uniform prior in this case can be supported with two arguments. First, for a variable with a restricted range like ϕ, a uniform prior is often considered non-informative in Bayesian terms [21]. Second, although it is known experimentally that ϕ is likely to have a low-curvature structure [9,10,16], the estimators we are considering assume that each pixel's parameters are independent. With this restriction, based on experimental results it is approximately equally likely that a single pixel chosen at random could have any value for ϕ in the valid range.

Proceeding with the uniform prior, we can then write

$$p(\boldsymbol{r}, \boldsymbol{\theta}; s) = \int_{-\pi}^{\pi} p(\boldsymbol{r}, \boldsymbol{\theta}; s, \phi) p(\phi) \, \mathrm{d}\phi \, . \tag{16}$$

We first note that

$$p(\boldsymbol{r}, \boldsymbol{\theta}; s, \phi) p(\phi) = \frac{1}{2\pi} \prod_{i=1}^{n} \frac{r_i}{2\pi\sigma^2} \exp\left(-\frac{s^2 + r_i^2 - 2 s r_i \cos(\theta_i - \phi)}{2\sigma^2}\right) . \tag{17}$$

Then we can substitute this in and simplify to produce

$$\begin{aligned} p(\boldsymbol{r}, \boldsymbol{\theta}; s) &= \frac{1}{2\pi} \int_{-\pi}^{\pi} \prod_{i=1}^{n} \frac{r_i}{2\pi\sigma^2} \exp\left(-\frac{s^2 + r_i^2 - 2 s r_i \cos(\theta_i - \phi)}{2\sigma^2}\right) \mathrm{d}\phi \\ &= \exp\left(-\frac{n s^2}{2\sigma^2}\right) \left(\prod_{i=1}^{n} \frac{r_i}{2\pi\sigma^2} \exp\left(-\frac{r_i^2}{2\sigma^2}\right) \right) \mathrm{I}_0\left(\frac{s\sqrt{A^2 + B^2}}{\sigma^2}\right) . \end{aligned} \tag{18}$$

We can then write the score function as

$$\frac{\mathrm{d}}{\mathrm{d}s}\log L(s;\boldsymbol{r},\boldsymbol{\theta}) = \frac{1}{\sigma^2}\left(\sqrt{A^2+B^2}\frac{\mathrm{I}_1\left(\frac{s\sqrt{A^2+B^2}}{\sigma^2}\right)}{\mathrm{I}_0\left(\frac{s\sqrt{A^2+B^2}}{\sigma^2}\right)} - ns\right). \tag{19}$$

This can be set equal to zero and solved for s using the same approach as in the previous section. The only difference between this new estimator and the one in the previous section is that this approach first averages the measurements together before applying the previous estimator.

3.4 Maximum Profile Likelihood Estimate with Saddlepoint Correction

In section 3.1 we saw that the maximum profile likelihood estimate is $\hat{s}_{\mathrm{ML}} = \frac{1}{n}\sqrt{A^2+B^2}$. One approach to removing the bias from this estimate involves a form of a technique called saddlepoint correction [19]. Using this approach, we compute a correction to the score function, equation (8), and then set the corrected score to zero and solve for our estimate. In our problem, the correction suggested by Levin *et al.* is given by [19]

$$\frac{\mathrm{d}}{\mathrm{d}s}\log L(s;\hat{\phi}_{\mathrm{ML}},\boldsymbol{r},\boldsymbol{\theta}) + B = 0\,. \tag{20}$$

with

$$\begin{aligned} B &= -\frac{\sigma^2}{2ns^2}E\left(\frac{\partial}{\partial s}\frac{\partial^2}{\partial\phi^2}\log p(\boldsymbol{r},\boldsymbol{\theta}\,;\,s,\phi)\right) \\ &= -\frac{1}{2s}\,. \end{aligned} \tag{21}$$

Setting the corrected profile score function to zero and solving for s gives the maximum corrected profile likelihood estimate

$$\hat{s}_{\mathrm{Corr}} = \frac{\hat{s}_{\mathrm{ML}} + \sqrt{\hat{s}^2_{\mathrm{ML}} - 2\sigma^2/n}}{2}\,, \tag{22}$$

where $\hat{s}_{\mathrm{ML}}$ is the uncorrected profile likelihood estimate as defined in section 3.1. This corrected estimator raises a difficulty when $\hat{s}^2_{\mathrm{ML}} < 2\sigma^2/n$ as our estimate becomes complex valued. We will resolve this by taking the real part as the estimate.

4 Other Published Estimators

In addition to the estimators derived above, there are several others that are significant in the MRI literature. A variety of previous approaches to reducing bias in magnitude MRI images are all based on noting that [1,3,4,5,8]

$$E[r_i^2] = s^2 + 2\sigma^2\,. \tag{23}$$

The estimator proposed independently by McGibney *et al.* and Miller *et al.* was created by replacing $E[r_i^2]$ with r_i^2 in this equation, and then solving for s, giving (in the general case with n measurements) [4,5]

$$\hat{s}_{\mathrm{MM}} = \sqrt{\frac{1}{n}\sum_{i=1}^{n} r_i^2 - 2\sigma^2}\,. \tag{24}$$

As with the corrected profile likelihood estimate, we take the real component of equation (24) as the estimated value. Practically, this means setting $\hat{s}_{\mathrm{MM}} = 0$ whenever $\frac{1}{n}\sum_{i=1}^{n} r_i^2 < 2\sigma^2$.

The estimator proposed by Gudbjartsson *et al.* is quite similar. Starting with just the Rician-distributed magnitude measurements, they propose to make the resulting estimator's distribution closer to Gaussian by using [1]

$$\tilde{s}_{\mathrm{G}} = \sqrt{\left|\frac{1}{n}\sum_{i=1}^{n} r_i^2 - \sigma^2\right|}\,. \tag{25}$$

With the introduction of the absolute value inside the square root, we are guaranteed a real-valued estimate.

Lastly, the estimator due to Koay *et al.* was designed for the situation where σ is unknown and may vary between pixels [8]. Since, for the purposes of our experiment, we assume that σ is known or can be estimated well and further that it is fixed for all pixels, we will not consider this estimator further.

5 Comparison of Estimators

5.1 Methods

It is hypothesized that the spatially varying bias of magnitude MRI images causes difficulties for observers [12,22]. This is assumed to be due to the reduction in image contrast. Bright image regions have essentially zero bias in magnitude images while dark regions are biased positively. Experiments involving human observers looking at biased and unbiased MRI images indicates that bias may hamper detection of dim features against a dark background (e.g., weak edges) [23]. Additionally, we assume that the variance of an estimator likely has some impact on detectability as well. Noting this, we will compare estimators both in terms of bias and MSE.

To perform these comparisons, we used Monte Carlo experiments under a series of realistic conditions, similar to those presented by Sijbers *et al.*[6,7] since we do not have analytic forms for the MSE and bias of the estimators. The one exception to this was the MLE, where the bias and MSE are given in equations (9) and (10) and so are simply evaluated directly. The experiments were conducted with signals between 0 and 4 at intervals of 0.25 with noise fixed at $\sigma = 1$. We tried each signal value with one, two, and four simulated excitations. In order to ensure a low error in our experiment, we ran 20,000 iterations of each condition for use in computing the relevant statistics.

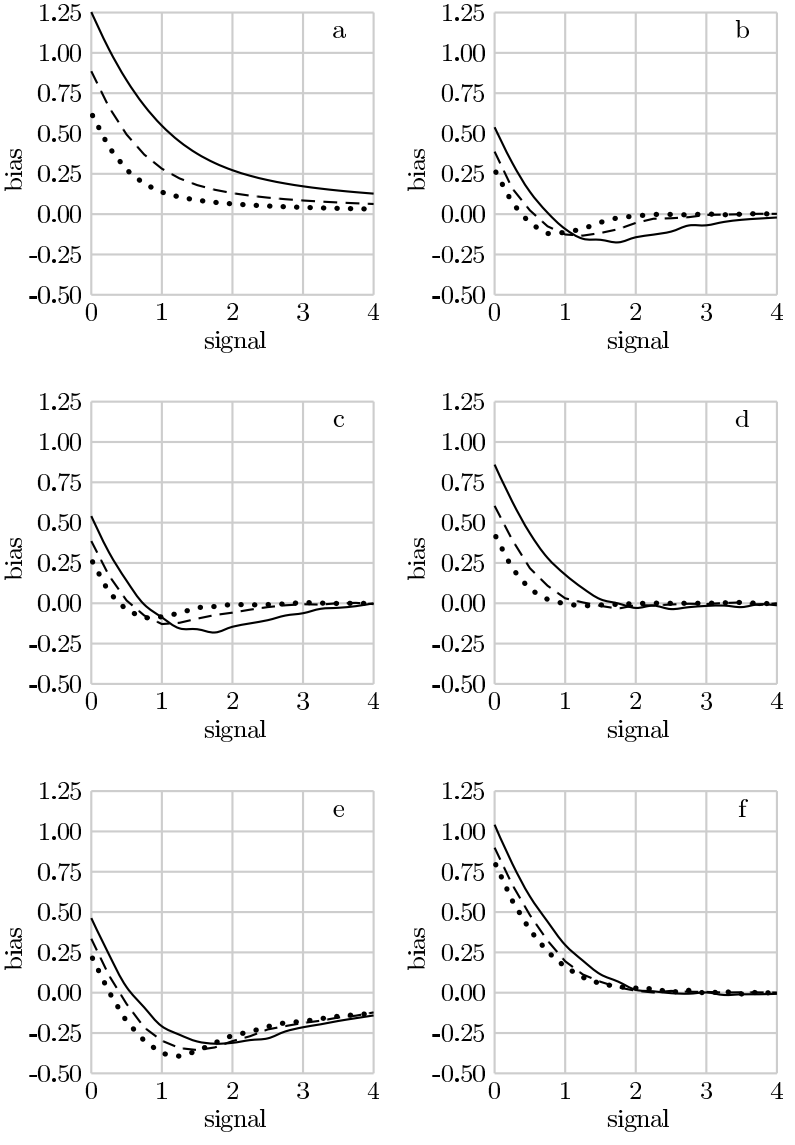

Fig. 1. Biases of the estimators. Each plot displays the bias of one estimator (a: maximum likelihood, b: maximum marginal likelihood, c: maximum integrated likelihood, d: maximum saddlepoint corrected profile likelihood, e: McGibney *et al.* and Miller *et al.*, f: Gudbjartsson *et al.*). The x-axis is the true signal value, and the y-axis is the mean bias of the estimate either computed directly or via the Monte Carlo experiments. The three lines in each plot correspond to $n = 1$ (solid), $n = 2$ (dashed), and $n = 4$ (dotted).

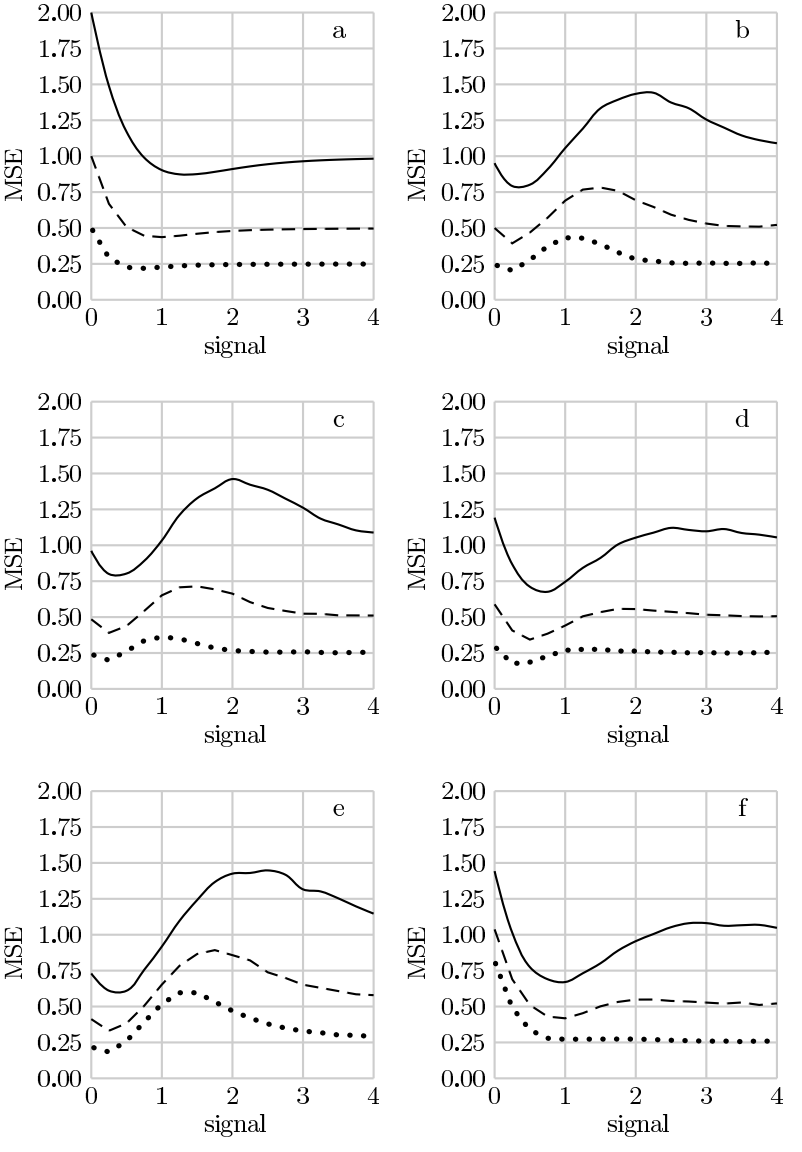

Fig. 2. MSEs of the estimators. Each plot displays the MSE of one estimator (a: maximum likelihood, b: maximum marginal likelihood, c: maximum integrated likelihood, d: maximum saddlepoint corrected profile likelihood, e: McGibney *et al.* and Miller *et al.*, f: Gudbjartsson *et al.*). The x-axis is the true signal value, and the y-axis is the MSE of the estimate either computed directly or via the Monte Carlo experiments. The three lines in each plot correspond to $n = 1$ (solid), $n = 2$ (dashed), and $n = 4$ (dotted).

5.2 Results and Discussion

In figure 1, we show the bias results. We can see that the McGibney *et al.* and Miller *et al.* estimate (e), along with the integrated and marginal likelihood estimators (b, c) are the least biased when the signal is 0. However, the corrected profile likelihood (d) is the most quick to converge to having no bias as the true signal increases. We note as the number of excitations increases the integrated likelihood estimate improves more rapidly than the marginal likelihood estimate. However, the corrected profile likelihood estimate converges to zero bias more quickly than the others with one, two, or four excitations.

In figure 2, we show the MSE results. The maximum likelihood estimate (a) produces the lowest MSE once $s > 1.5$. The next closest estimators are the corrected profile likelihood (d) and the Gudbjartsson *et al.* estimator (f). For signal values approaching 0, the McGibney *et al.* and Miller *et al.* estimator has the lowest MSE, followed by the integrated and marginal likelihood estimators (b, c). Again we note that the MSE of the integrated likelihood estimate improves more rapidly than the marginal likelihood estimate. Additionally, we find that the corrected profile likelihood estimate becomes increasingly competitive with the integrated and marginal likelihood estimates in terms of MSE as the number of excitations increases.

Considering these results together, our experiments suggest that the corrected profile likelihood estimate (d) provides less bias than the maximum likelihood estimate while trading a lower MSE at $s < 1.5$ for a slightly higher MSE at $s > 1.5$. These results seem to indicate that this new estimator offers a competitive alternative to those already published.

One practical consideration is the computational costs of these estimators. The marginal and integrated likelihood estimates both require several steps of some optimization algorithm. Although an efficient optimization algorithm for this problem has been previously presented [6], they are still substantially more expensive to compute than the the maximum corrected profile likelihood, McGibney *et al.* and Miller *et al.*, or Gudbjartsson *et al.* estimators. As such, we suspect that in a practical setting, the benefits achieved by applying the maximum corrected profile likelihood estimator could be sufficient to offset the minimal computational cost required for every image.

6 Conclusions

We have demonstrated that a variety of estimators for MRI, both previously published and new, can be generated by applying some of the statistical approaches to maximum likelihood estimation in the presence of nuisance parameters. Our results suggest that the rich literature on this type of problem in statistics offers useful tools that can be applied to signal estimation in MRI.

As there is no clear theoretical grounds for choosing one of these estimators, we have used Monte Carlo experiments to compare the estimators. We have shown that a novel MRI signal estimator, the maximum corrected profile likelihood,

offers a decrease in bias compared to the magnitude image, in exchange for a slight increase in variance. Additionally, our results suggest that in situations with multiple excitations there can be substantial advantage to using this new estimator. Due to the limitations of the metrics being used for the evaluations, the results can only be considered to suggest further work. Experiments with humans observing estimated images are necessary to determine if any of these estimators provide a practical improvement in MR images.

Acknowledgments

The authors would like the Natural Sciences and Engineering Research Council of Canada for their support of this work.

References

1. Gudbjartsson, H., Patz, S.: The Rician distribution of noisy MRI data. Magn. Reson. Med. 34, 910–914 (1995)
2. Macovski, A.: Noise in MRI. Magn. Reson. Med. 36, 494–497 (1996)
3. Henkelman, R.M.: Measurement of signal intensities in the presence of noise in MR images. Med. Phys. 12(2), 232–233 (1985)
4. McGibney, G., Smith, M.R.: An unbiased signal-to-noise ratio measure for magnetic resonance images. Med. Phys. 20(4), 1077–1078 (1993)
5. Miller, A.J., Joseph, P.M.: The use of power images to perform quantitative analysis on low SNR MR images. Magn. Reson. Imaging 11, 1051–1056 (1993)
6. Sijbers, J., den Dekker, A.J., Scheunders, P., Dyck, D.V.: Maximum-likelihood estimation of Rician distribution parameters. IEEE Trans. Med. Imag. 17(3), 357–361 (1998)
7. Sijbers, J., den Dekker, A.J.: Maximum likelihood estimation of signal amplitude and noise variance from mr data. Magn. Reson. Med. 51, 586–594 (2004)
8. Koay, C.G., Basser, P.J.: Analytically exact correction scheme for signal extraction from noisy magnitude MR signals. J. Magn. Reson. 179, 317–322 (2006)
9. Ahn, C.B., Cho, Z.H.: A new phase correction method in NMR imaging based on autocorrelation and histogram analysis. IEEE Transactions on Medical Imaging 6(1), 32–36 (1987)
10. Bernstein, M.A., Perman, W.H.: Least-squares algorithm for phasing MR images. In: Book of Abstracts vol. 2, p. 801. In: Sixth Annual Meeting of SMRM, Society of Magnetic Resonance in Medicine August 1987 (1987)
11. Noll, D., Nishimura, D., Macovski, A.: Homodyne detection in magnetic resonance imaging. IEEE Trans. Med. Imag. 10, 154–163 (1991)
12. Nowak, R.D.: Wavelet-based Rician noise removal for magnetic resonance imaging. IEEE Trans. Image Processing 8(10), 1408–1418 (1999)
13. Alexander, M.E., Baumgartner, R., Summers, A.R., Windischberger, C., Klarhoefer, M., Moser, E., Somorjai, R.L.: A wavelet-based method for improving signal-to-noise ratio and contrast in MR images. Magn. Reson. Imaging 18, 169–180 (2000)
14. Bao, P., Zhang, L.: Noise reduction for magnetic resonance images via adaptive multiscale products thresholding. IEEE Trans. Med. Imag. 22(9), 1089–1099 (2003)
15. Tisdall, M.D., Atkins, M.S.: MRI denoising via phase error estimation. In: Proc. SPIE. vol. 5747, pp. 646–654 (2005)

16. Chang, Z., Xiang, Q.S.: Nonlinear phase correction with an extended statistical algorithm. IEEE Trans. Med. Imag. 24(6), 791–798 (2005)
17. Bartlett, M.S.: Approximate confidence intervals: III a bias correction. Biometrika 42(1/2), 201–204 (1955)
18. Kalbfleisch, J.D., Sprott, D.A.: Application of likelihood methods to models involving large numbers of parameters. Journal of the Royal Statistical Society B 32(2), 175–208 (1970)
19. Levin, B., Kong, F.: Bartlett's bias correction to the profile score function is a saddlepoint correction. Biometrika 77(1), 219–221 (1990)
20. Liang, K.Y., Zeger, S.L.: Inference based on estimating functions in the presence of nuisance parameters. Statistical Science 10(2), 158–173 (1995)
21. Jeffreys, H.: Theory of Probability, 3rd edn. Claredon Press (1961)
22. Bernstein, M.A., Thomasson, D.M., Perman, W.: Improved detectability in low signal-to-noise ratio magnetic resonance images by means of a phase-corrected real reconstruction. Med. Phys. 16, pp. 813–817 (1989)
23. Tisdall, M.D., Atkins, M.S.: Perception of dim targets on dark backgrounds in MRI. In: SPIE Medical Imaging 2007, Proceedings of 2007 (2007)